While the angle factor F^{DD} between these two disks is defined as

$$q = \frac{\pi D_T^2}{4} F^{DD} \sigma T^4 \qquad \text{(A 20)}$$

Finally from Eqs.(A 19), (A 20) and (A 14), one obtains

$$F^{DD} = \frac{4}{\pi}\int_{-\pi/2}^{\pi/2} \cos\theta d\theta \int_0^{\cos\theta} dz \int_0^{\tan^{-1} z/x'} e^{-Cx'/\cos\phi} \times \sin\phi\cos\phi d\phi \qquad \text{(A 21)}$$

Angle factors f^{RR}, F^{RD} and F^{DD} are calculated numerically as function of x' with the parameter ε_G, and shown in **Figs. 9, 10,** and **11,** respectively. When $C=0$ ($\varepsilon_G=0$), Eqs.(A 7), (A 15) and (A 21) can be integrated analytically into the forms derived by Hottel[3].

Nomenclature

$B = HL/C_pGT_0$, dimensionless rate of heat generation [—]
$C = kD_T$ [—]
C_p = specific heat of gas [kcal/kg·°C]
$D = L/D_T$ [—]
D_T = tube diameter [m]
E = longitudinal fluid mixing coefficient [m²/hr]
F^{DD} = angle factor between two circular cross sections of tube, cotaining gray gas [—]
F^{RD} = angle factor from ring element on tube inside wall to circular cross section of tube, cotaining gray gas [—]
F^{RR} = angle factor between two ring elements on tube inside wall, containing gray gas [—]
f = Fanning friction factor [—]
$f^{RR} = F^{RR}/dx'$ [—]
G = mass velocity of gas [kg/m²·hr]
H = rate of heat generation [kcal/m³·hr]
K_e = effective thermal conductivity of gas, $K_r + K_{mix} + K_G$ [kcal/m·hr·°C]
K_G = molecular thermal conductivity of gas [kcal/m·hr·°C]
K_{mix} = longitudinal conductivity due to fluid mixing [kcal/m·hr·°C]
K_r = radiant conductivity [kcal/m·hr·°C]
k = absorption coefficient [m⁻¹]
L = tube length [m]
l = distance variable [m]
M, N = constants, $B = N + Mt$ [—]
N_{Pr} = Prandtl number [—]
N_{Re} = Reynolds number [—]
Q_1 = radiation flux in forward direction [kcal/m²·hr]
Q_2 = radiation flux in backward direction [kcal/m²·hr]
q_w = radiation energy arriving at wall surface element [kcal/m²·hr]
r = distance variable [m]
S = area [m²]
s = distance variable [m]
T = temperature [°K]
T_0 = inlet temperature of gas [°K]
$t = T/T_0$ [—]
u = linear gas velocity [m/hr]
$x = l/L$ [—]
$x' = l/D_T$ [—]
y_1 = dimensionless radiation flux in forward direction, $Q_1/\sigma T_0^4$ [—]
y_2 = dimensionless radiation flux in backward direction, $Q_2/\sigma T_0^4$ [—]
$z = s/D_T$ [—]

Greek letters

α = dimensionless parameter, $\sigma T_0^3/C_pG$ [—]
β = angie variable [—]
ε_G = emissivity of gas [—]
θ = angle variable [—]
σ = Stefan-Boltzmann constant, 4.88×10^{-8} [kcal/m²·hr·°K⁴]
ρ = density of gas [kg/m³]
ϕ = angle variable [—]
ψ = angle variable [—]

Literature cited

1) Chen, J. C. and S. W. Churchill: *A. I. Ch. E. Journal*, **9**, 35 (1963)
2) Hamaker, H. C.: *Philips Research Repts.*, **2**, 55, 103, 112, 420 (1947)
3) Hottel, H. C.: "Geometrical problems in radiant heat transfer", Heat Transfer Lectures, Vol. II, NEPA-979, I. E. R.-13. Fairchild Corp., Oak Ridge (1949)
4) Hottel, H. C. and E. S. Cohen: *A. I. Ch. E. Journal*, **4**, 3 (1958)
5) Hottel, H. C., A. F. Sarofim and C. Takeuchi: *Kagaku Kōgaku* **26**, 962 (1962)
6) McAdams, W. H.: "Heat Transmission", 3ed., McGraw-Hill, New York (1954).
7) Taylor, G. I.: *Proc. Roy. Soc.*, **223 A**, 446 (1954)

HEAT TRANSFER FROM WALL SURFACE TO PACKED BEDS AT HIGH REYNOLDS NUMBER*

DAIZO KUNII, MOTOYUKI SUZUKI AND NAOSHI ONO**

Department of Chemical Engineering, University of Tokyo, Tokyo

Introduction

Prediction of the heat transfer rate between wall surface and packed beds is of particular importance in connection with the rational design of catalytic reactors, especially in case of chemical reactions accompanied by great deal of heat generation or absorption.

The authors[3] have analysed the mechanism of heat transfer between wall and packed solids, introducing the following equation

$$\frac{h_w D_p}{k_f} = 2.0 \frac{1}{\frac{1}{k_{ew}/k_f} - \frac{1}{k_{er}/k_f}} \qquad (1)$$

where h_w represents the apparent heat transfer coefficient on the wall. Then k_{er} and k_{ew} mean the effective thermal conductivity in the interior of the bed and that

* Received on July 3, 1967

** Showa Denko Co., Ichihara

in the "near-wall region" which is defined as 1/2-particle-diameter interval from the wall, respectively.

In the range of low Reynolds number ($Re_p \ll 10^3$ for gaseous system), the effective thermal conductivity k_{ew} in the vicinity of wall surface is described by the following equation

$$\frac{k_{ew}}{k_f} = \frac{k_{ew}^0}{k_f} + \alpha_v \left(\frac{C_p \mu}{k_f}\right)\left(\frac{D_p G_0}{\mu}\right) \tag{2}$$

The first term of the R. H. S. of the above equation represents the contribution of conduction and radiation between wall and contacting solids, while the second term corresponding to the effect of fluid mixing in the direction normal to the wall in the vicinity of wall surface. The value of α_v is determined to be about 0.02 by application of random walk concept near the wall surface. This equation was verified experimentally in the wall previous paper[3] in the range $Re_p < 500$ for air system. When the velocity of fluid increases in packed beds, the contribution of thermal boundary layer may dominate the heat transfer mechanisms near the wall surface. In literatures, however, there have been reported few data in connection with the heat transfer mechanisms between wall surface and packed beds especially for high Reynolds numbers, i. e. $Re_p \gg 10^3$.

The authors[4] made an experimental work on mass transfer between the wall surface and flowing water in paked beds in order to clarify the behavior of the boundary layer on the wall surface, utilizing the fact the resistance of the boundary layer may be the controlling step in a system of high Schmidt number. In fully turbulent region ($Re_p \gg 10^2$), the wall mass transfer coefficients were correlated in the previous paper[4] as the form of Blasius equation,

$$\frac{K_w D_p}{D_v} = C\left(\frac{\nu}{D_v}\right)^{1/3}\left(\frac{D_p G_0}{\mu}\right)^{3/4} \tag{3}$$

$$C = 0.06 \cdot \varepsilon_w^{-2} \tag{3'}$$

The wall mass transfer coefficient K_w corresponds to the heat transfer coefficient of the thermal boundary layer, h_w^*. Then h_w^* might be estimated from the following equation

$$\frac{h_w^* D_p}{k_f} = C\left(\frac{C_p \mu}{k_f}\right)^{1/3}\left(\frac{D_p G_0}{\mu}\right)^{3/4} \tag{4}$$

Conduction of heat through the thermal boundary layer and convection due to the fluid mixing may be considered as successive mechanisms as shown in **Fig. 1.**

Then the effective thermal conductivities in the near-wall region, k_{ew}, can be simply formulated as follows:

$$\frac{k_{ew}}{k_f} = \frac{k_{ew}^0}{k_f} + \frac{1}{\dfrac{1}{\alpha_v Pr Re_p} + \dfrac{1}{h_w^* D_p / 2k_f}} \tag{5}$$

Yagi and Wakao[9] reported a correlation for apparent heat transfer coefficients at the wall in terms of Colburn's equation in the range $40 < Re_p < 800$,

$$\frac{h_w D_p}{k_f} = 0.2\left(\frac{C_p \mu}{k_f}\right)^{1/3}\left(\frac{D_p G_0}{\mu}\right)^{0.8} \tag{6}$$

Though their heat transfer experiment was made under the condition where the resistance of fluid mixing could be dominant the above correlation suggests the development of turbulent boundary layers on the wall surface.

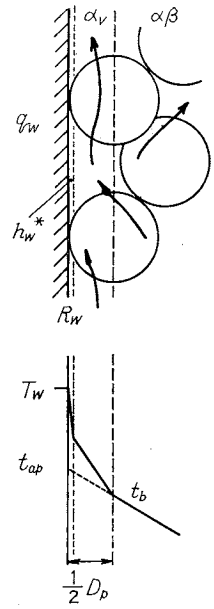

$$q_w = k_{er}\frac{\partial t}{\partial r}\Big| r = R_W - \frac{1}{2}D_p$$
$$= h_w(T_w - t_{ap})$$
$$= \frac{k_{ew}}{\frac{1}{2}D_p}(T_w - t_b)$$

Fig. 1 Model of heat transfer near the wall surface

"Near-wall region"

Experiment

Apparatus and procedure

Fig. 2 shows the schematic diagram of the experimental set up. A main column consisted of three units of copper cylinders of 140 mm I. D. fitted together with flanges. The first one of the three cylinders of 200 mm in length was used as a calming section followed by test section of 600 mm in length made of two units. The wall of the test section was heated up to 100°C by steam jackets. Air was introduced to the bottom of the column and passed upwards through the calming section where uniform flow patterns were obtained.

Temperature profiles at the center axis and at the exit section of the test section were determined with 0.3 mmϕ Alumel-Chromel thermocouples. Some of the thermocouples were settled between parcicles with bamboo stick supports, while the others were embedded in particles by epoxy resin. Thermoelectric powers were measured by Potentiometer P-31A by Yokogowa Elec. Co. to an accuracy of 0.1°C after confirmation of steady state by means of an auto-potentiometric recorder.

Flow rates of air were measured by a calibrated orifice flowmeter. The range of flow rates of air was 12~580 kg/hr. Two different sizes of celite spheres (28 mmϕ and 42 mmϕ) were employed as packings. Average void fraction in the bed was determined by counting numbers of particles packed in the test section, which was 0.532 or 0.545 respectively for two sizes i. e., D_p=28 mm or 42 mm.

Analysis

There were nearly no significant difference between the temperature profiles measured by thermocouples embedded in particles and those by thermocouples settled in the void spaces under the present experimental conditions. Therefore, successive analysis can be made on the assumption that there is no temperature difference between solids and flowing fluid.

Then the basic equation is

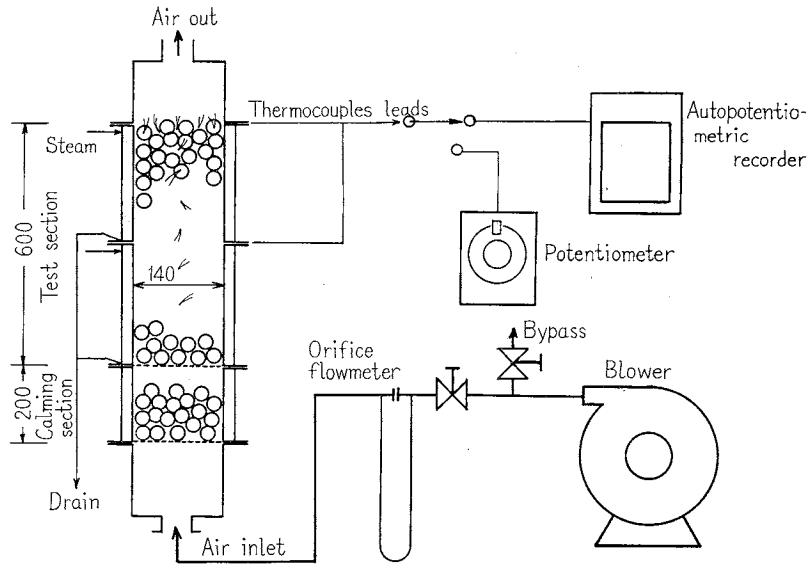

Fig. 2 Schematic diagram of experimental apparatus

$$C_pG_0\frac{\partial t}{\partial z}=k_{ez}\frac{\partial^2 t}{\partial z^2}+k_{er}\left(\frac{\partial^2 t}{\partial r^2}+\frac{1}{r}\frac{\partial t}{\partial r}\right) \tag{7}$$

Boundary conditions are

$$\left.\begin{aligned} &z=0:\ t=t_0\\ &r=R_w:\ k_{er}\frac{\partial t}{\partial r}=h_w(T_w-t)\end{aligned}\right\} \tag{8}$$

Axial conduction can be neglected at such high Reynolds numbers as in the present work and a solution for semi-infinite cylinder can be applied for $k_{ez}/k_{er}<10^{5)}$. Then the temperature distribution may be written as

$$\frac{T_w-t}{T_w-t_0}=\sum_{i=1}^{\infty}\frac{bJ_0(\xi a_i)\exp(-\kappa a_i^2\eta)}{(b^2+a_i^2)J_0(a_i)} \tag{9}$$

where a_i is the i th positive root of the following equation

$$b=a_iJ_1(a_i)/J_0(a_i) \tag{10}$$

where

$$b=h_wR_w/k_{er} \tag{11}$$

and

$$\kappa=k_{er}/C_pG_0R_w \tag{12}$$

$$\xi=r/R_w,\qquad \eta=z/R_w$$

When the bed is long enough $(\kappa\cdot\eta>0.2)$, Eq. (9) is approximated by the first term in the series

$$\frac{T_w-t}{T_w-t_0}=\frac{bJ_0(\xi a_1)\exp(-\kappa a_1^2\eta)}{(b^2+a_1^2)J_0(a_1)} \tag{13}$$

Temperature profile at the exit section of the bed $t_e(\xi)$ is expressed simply in terms of temperature at the center of the section t_{ec}

$$\frac{T_w-t_e}{T_w-t_{ec}}=J_0(a_1\xi) \tag{14}$$

And temperature distribution along the center axis in the bed t_c is given[1] as

$$\frac{T_w-t_c}{T_w-t_0}=\frac{b}{b^2+a_1^2}\cdot\frac{\exp(-\kappa a_1^2\eta)}{J_0(a_1)} \tag{15}$$

and then

$$\log\left(\frac{T_w-t_c}{T_w-t_0}\right)=-\kappa a_1^2\eta+\text{const} \tag{15'}$$

From the radial temperature profile measured at the exit section a_1 is calculated by means of Eq. (14). On the other hand semi-log plot of temperatures at the center axis against non-dimensional longitudinal position η gives the gradient $(-\kappa a_1^2)$. Then the value of κ is calculated by substitution of a_1 obtained before and then k_{er} and h_w are given from Eqs. (10) ~ (12).

Apparent overall heat transfer coefficients are calculated from the following equation

$$h_0=\frac{C_pG_0\Delta t\cdot\pi R_w^2}{\Delta t_{l.m.}2\pi R_wL} \tag{16}$$

where Δt is a mean temperature rise of fluid throughout the bed and $\Delta t_{l.m.}$ denotes logarithmic mean temperature difference between wall and fluid. These two values can be determined from the temperature distribution at the exit section $t_e(\xi)$, as follows

$$\Delta t=\bar{t}_e-t_0 \tag{17}$$

$$\Delta t_{l.m.}=\Delta t/\ln\left(\frac{\bar{t}_e-T_w}{t_0-T_w}\right) \tag{18}$$

$$\bar{t}_e=2\int_0^1 t_e(\xi)\cdot\xi\cdot d\xi \tag{19}$$

Results and Discussions

The effective thermal conductivities calculated from the measured temperature profiles are plotted against particle Raynolds numbers, D_pG_0/μ, in **Fig. 3.** The figure shows the validity of Yagi and Kunii equation in the condition of the present experiment

$$\frac{k_{er}}{k_f}=\frac{k_e^0}{k_f}+(\alpha\beta)\left(\frac{C_p\mu}{k_f}\right)\left(\frac{D_pG_0}{\mu}\right) \tag{20}$$

Theoretical value of k_e^0/k_f calculated from Kunii and Smith's Eq. (1) for 28mm spheres is 14.0, which is included in Fig. 3.

The amount of $\alpha\beta$ calculated from the slope of regression line in Fig. 3 is 0.12 for the both sizes of particles. This value seems to be a little larger than those expected from the previous studies[3,8].

The apparent heat transfer coefficients on the wall are shown in **Fig. 4.**

The effective thermal conductivities in the vicinity of the wall surface calculated from h_w and k_{er} by means of Eq. (1) are plotted in **Fig. 5.** The extrapolated value of k_{ew}/k_f from the flow condition to $Re_p=0$ is 8.0 which coincided fairly well with the theoretical value 9.0 calculated from Yagi and Kunii equation modified by the authors[3,7]. Solid line in Fig. 5 shows Eq. (2) which represents the contribution of convective transfer of

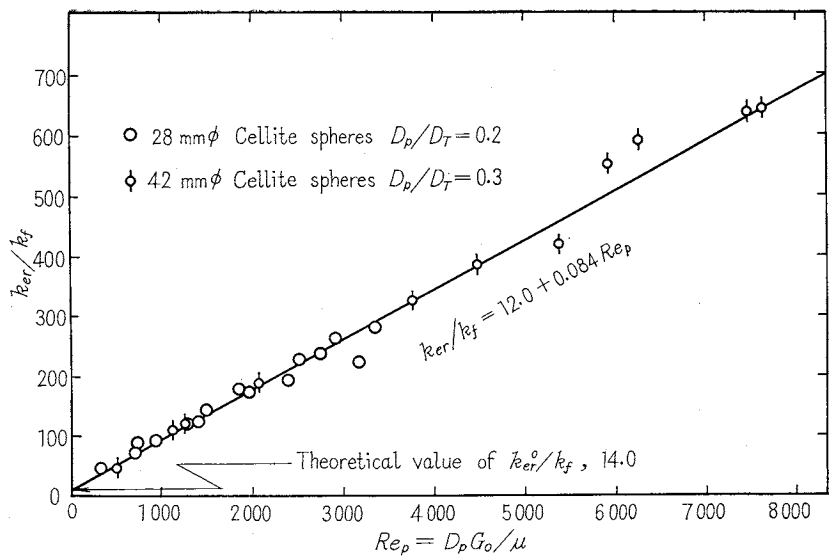

Fig. 3 Effective thermal conductivities in the radial direction

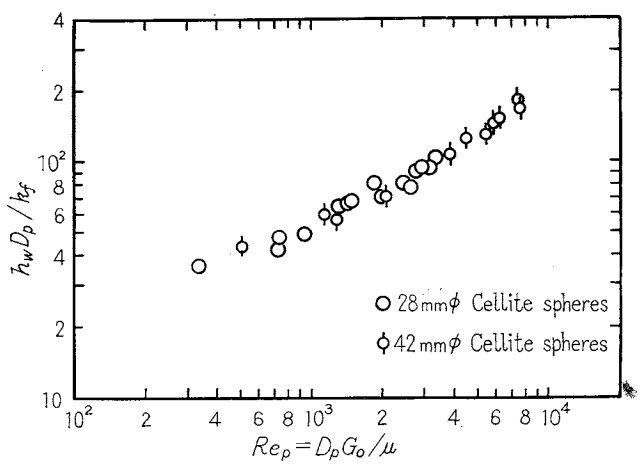

Fig. 4 Apparent heat transfer coefficients at the wall

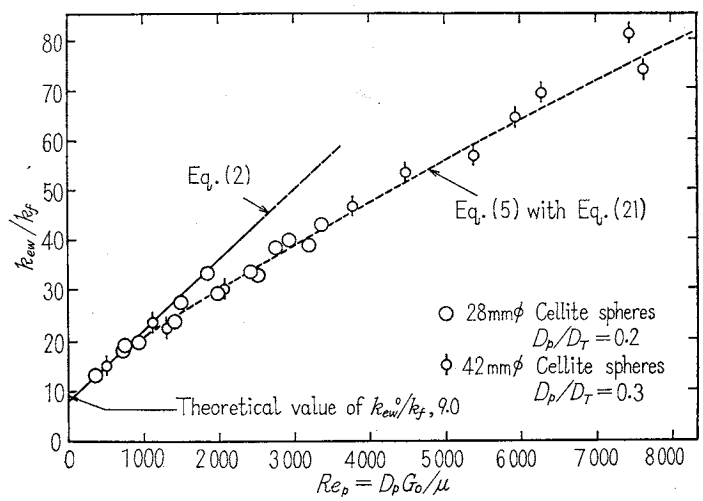

Fig. 5 Effective thermal conductivities in the near-wall region

heat in the near-wall region due to fluid mixing normal to the wall. It may be understood that Eq. (2) is reasonable at low Reynolds numbers ($Re_p \ll 10^3$). The data, however, deviate from Eq. (2) at high Reynolds numbers. This discrepancy may be due to the effect of thermal resistance of the boundary layer which will develop on the wall surface and be dominant at high Reynolds numbers. Then Eqs. (4) and (5) may be applicable to the heat transfer in the near-wall region. Much difficulty lies in determining the values of the coefficients C in Eqs. (3) and (4) from a model interpretation, since C may depend on many bed properties such as void fraction, not only in the vicinity of the wall but also in the interior of the bed, particle diameter to tower diameter ratio and so on. The authors[4] correlated the values of C obtained in the mass transfer experiments in two-dimensional packed beds of spheres by means of a semi-theoretical equation which is Eq. (3′). But as stated earlier, C may be a more complex function of the bed properties. So Eq. (3′) is to be restricted to a two-dimensional bed or a bed with small D_p/D_T ratio, where the variation of porosity near the wall may not affect the bed properties in the interior of the bed. Here the value of C is selected to interpret the experimental data of k_{ew}/k_f in terms of Eqs. (4) and (5). Thus selected values of C are shown against D_p/D_T in **Fig. 6**. In the present case Eq. (4) can be written as

$$\frac{h_w^* D_p}{k_f} = 0.5\left(\frac{C_p\mu}{k_f}\right)^{1/3}\left(\frac{D_pG_0}{\mu}\right)^{3/4} \tag{21}$$

Eq. (5) with (21) is indicated by a dotted line in Fig. 5, correlating the observed values of k_{ew}/k_f pretty well.

Apparent overall heat transfer coefficients, h_0, are shown in **Fig. 7**. According to Yagi and Kunii[7], h_0 is obtained from the following equation, in case $y = k_{er}L/C_pG_0R_w^2 > 0.2$

$$\frac{h_0D_p}{k_f} = \left(\frac{k_{er}}{k_f}\right)\left(\frac{D_p}{D_T}\right)\{a_1^2 + \phi(b)/y\} \tag{22}$$

$$\phi(b) = \ln\{a_1^2(1 + a_1^2/b^2)/4\} \tag{23}$$

where a_1 is the first positive root of the transcendental equation

$$b = a_1J_1(a_1)/J_0(a_1) \tag{10′}$$

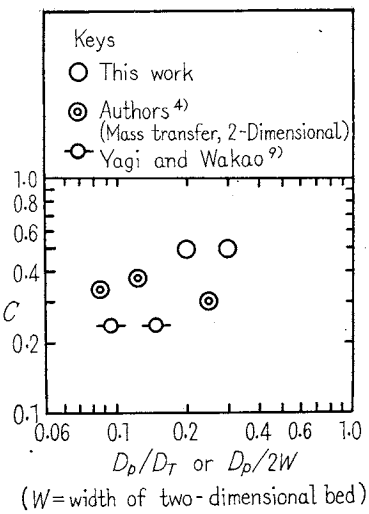

Fig. 6 Plots of experimentally obtained C against D_p/D_T

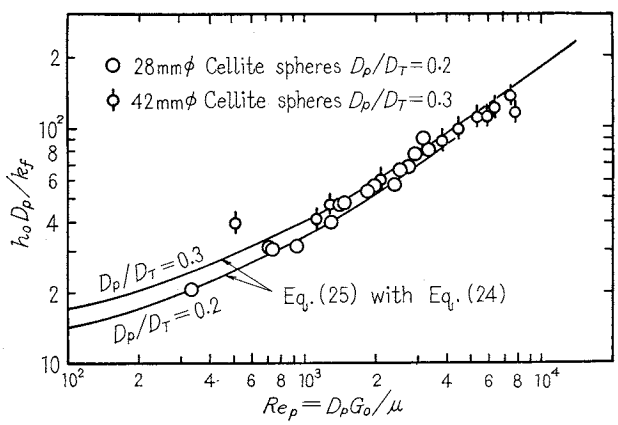

Fig. 7 Apparent overall heat transfer coefficients

And b is defined by Eq.(11). The relation between a_1^2 and b, that is Eq.(10'), has two asymptotes

$$\begin{cases} b \to 0 & a_1^2 = 2 \cdot b \\ b \to \infty & a_1^2 = 5.78 \end{cases}$$

These asymptotes suggests the approximate relation between a_1^2 and b, which is

$$a_1^2 = 5.78b/(b + 2.89) \tag{24}$$

Eq.(24) gives an approximate values of a_1^2 to an error less than 10%. This relation is useful for the rapid estimation of a_1^2 rather than Eq.(10').

And then from numerical studies Eq.(22) is simplified in the following manner.

(I) In the case $b<1.8$ which is satisfied at high Reynolds numbers or at large D_p/D_T values, only the first term in Eq.(22) is of practical significance and then

$$\frac{h_0D_p}{k_f} = \left(\frac{k_{er}}{k_f}\right)\left(\frac{D_p}{D_T}\right)a_1^2 \tag{25}$$

Furthermore at smaller values of $b(b<0.4)$ Eq.(24) gives $a_1^2=2b$ then Eq.(25) reduces to

$$h_0 = h_w \tag{26}$$

In this range of parameters, the heat transfer resistance in the interior of the bed is negligible in comparison with the resistance of heat transfer at the wall.

(II) On the other hand at high values of $b(b>20)$, a_1^2 is nearly equal to a constant value 5.78

$$a_1^2 \simeq 5.78 \tag{27}$$

Especially in the case $y \gg 0.64$, the second term in Eq.(22) is negligible and then

$$\frac{h_0D_p}{k_f} = 5.78\left(\frac{k_{er}}{k_f}\right)\left(\frac{D_p}{D_T}\right) \tag{28}$$

This equation shows that the heat transfer coefficient at the wall is not significant for the estimation of the apparent overall heat transfer coefficient in packed beds in this range of parameters.

The factor b is important in the above calculations, which is estimated directly from k_{ew} and k_{er} as follows

$$b = \frac{h_wR_w}{k_{er}} = \left(\frac{D_T}{D_p}\right)\left(\frac{k_{ew}/k_f}{k_{er}/k_f - k_{ew}/k_f}\right) \tag{29}$$

In the range of the present experiment, the values of b calculated from Eq.(29) is rather small. Then Eq.(25) with Eq.(24) can be applied and compared with the observed data. The solid lines in Fig. 7 represent the above approximate equation, which show a good agreement with the experimental data. These simple approximate procedures are helpful in the practical estimation of the apparent overall heat transfer coefficients.

Conclusion

Experimental works were made on heat transfer from steam-jacketed wall to flowing air in cylindrical packed beds for Reynolds number $Re_p=3\times10^2\sim8\times10^3$. In high Reynolds number range, the heat transfer resistance through boundary layer on the wall surface becomes effective. Effective thermal conductivities in the near-wall region, k_{ew}, is reasonably estimated from Eqs.(5) and (4) at high Reynolds numbers, while it is approximated by Eq.(2) at low Reynolds numbers ($Re_p \ll 10^3$ for gaseous system). Then apparent heat transfer coefficient, h_w, can be calculated from Eq.(1). Apparent overall heat transfer coefficient h_0 is compared with the approximate equation simplified from Yagi and Kunii's equation. Good coincidence indicates that the approximate equations are helpful for the practical estimation of the apparent overall heat transfer coefficients.

Nomenclature

a_i = i th positive root of Eq.(10)
b = $h_wR_w/k_{er} = (D_T/D_p)\,(k_{ew}/k_f/(k_{er}/k_f - k_{ew}/k_f))$
C = coefficient in Eqs.(3) and (4)
C_p = heat capacity of fluid [kcal/kg·deg]
D_p = diameter of particle [m]
D_T = diameter of tower [m]
D_v = molecular diffusivity [m²/h]
G_0 = superficial mass velocity of fluid [kg/m²h]
h_w = apparent heat transfer coefficient on the wall [kcal/m²·h·deg]
h_w^* = heat transfer coefficient of the boundary layer on the wall [kcal/m²·h·deg]
k_e^0 = effective thermal conductivity with stagnant fluid in the interior of a packed bed [kcal/m·h·deg]
k_{er} = effective thermal conductivity in the radial direction [kcal/m·h·deg]
k_{ew} = effective thermal conductivity in the near-wall region [kcal/m·h·deg]
k_{ew}^0 = effective thermal conductivity in the near-wall region with stagnant fluid [kcal/m·h·deg]
k_{ez} = effective thermal conductivity in the axial direction [kcal/m·h·deg]
k_f = thermal conductivity of fluid [kcal/m·h·deg]
K_w = mass transfer coefficient of the boundary layer on the wall [m/h]

L = length of test section [m]
r = distance in the radial direction [m]
Re_p = Reynolds number based on particle diameter $= D_p G_0/\mu$
R_w = radius of tower [m]
t = temperature [deg]
t_c = temperature at the center axis [deg]
t_e = temperature at the exit of the bed [deg]
t_0 = temperature at the inlet of the bed [deg]
t_{ap} = apparent wall temperature extrapolated from temperature profile in the interior [deg]
t_b = temperature at $r = R_w - \frac{1}{2}D_p$ [deg]
T_w = temperature at the wall [deg]
W = width of 2-dimensional bed [m]
y = $k_{er}L/C_pG_0R_w^2$
z = distance in the axial direction [m]

Greek Letters

$\alpha\beta$ = ratio of the rate of lateral movement of fluid to the flow rate in the interior of the bed
α_v = ratio of the rate of fluid displacement normal to the wall to the flow rate in the near-wall region
ε_w = void fraction in the near-wall region
ξ = nondimensional radial distance $= r/R_w$
η = nondimensional axial distance $= z/R_w$
κ = $k_{er}/C_pG_0R_w$
μ = viscosity of fluid [kg/m·h]
ν = kinematic viscosity of fluid [m²/h]

Literature cited

1) S. Hatta and S. Maeda: *Kagaku Kikai*, **12**, 56 (1948)
2) D. Kunii and J.M. Smith: *A. I. Ch. E. Jl.*, **6**, 97 (1960)
3) D. Kunii and M. Suzuki: Int. Heat Transfer Conference (Chicago) IV, 334 (1966)
4) D. Kunii and M. Suzuki: paper presented to Sympo. Heat Mass Transfer (Minsk) (1968)
5) N. Wakao and S. Yagi: *Kagaku Kōgaku*, **23**, 161 (1959)
6) S. Yagi and D. Kunii: *Kagaku Kōgaku*, **18**, 576 (1954); *A. I. Ch. E. Jl.*, **3**, 373 (1957)
7) S. Yagi and D. Kunii: Int. Devel. Heat Transfer, IV, 742 (1961)
8) S. Yagi, D. Kunii and N. Wakao: Int. Devel. Heat Transfer IV, 750 (1961)
9) S. Yagi and N. Wakao: *A. I. Ch. E. J.*, **5**, 79 (1959)

ON THE MECHANISM OF DRYING OF GRANULAR BEDS

—— Mass Transfer from Discontinuous Source* ——

MUTSUMI SUZUKI AND SIRO MAEDA

Dept. of Chem. Eng., Tohoku Univ., Sendai

Introduction

In the course of drying of wet granular materials, a period of constant drying rate is observed in most cases. It is usually stated that the rate of evaporation from the beds of such fine granular materials as clay is equal to that from a free water surface during the period of constant rate. In the case of relatively coarse granular materials such as sand, however, it was shown by Ceaglske[1] that these rates are slightly different each other. Shishkov[2] also reported that such an equality did not hold under a severe drying condition. Nevertheless, difference between the above two rates of evaporation is sufficiently small for granular materials of practical interest. In explaining the constant drying rate, it has been assumed that the ratio of wet surface area to the sectional area of the beds remains constant during the concerned period, even though the moisture concentration decreases and pores at the surface increase with the time elapse. In most cases it has also been assumed that the surface of granular material is completely covered with a water film during this period.

In the drying of granular, non-hygroscopic materials such as sand or glass spheres, liquid water within the beds is drawn to the evaporating plane by a capillary action. The menisci at the surface must then have smaller radii of curvature than those in the interior of the beds, and there may be a dried region above each surface of the non-hygroscopic solid particles as shown in **Fig. 1**. The water evaporating from the surface is necessarily replaced by the air which enters the beds through large pores at the surface, and then there must be vacant pores at the surface of the solids being dried.

In other words, the evaporation takes place from the discontinuous menisci at the surface of the beds during the constant drying rate period, the ratio of the area of the menisci to the drying surface decreases with decreasing surface moisture concentration.

Heat and mass transfer from such a discontinuous source also occur in the other unit operations such as

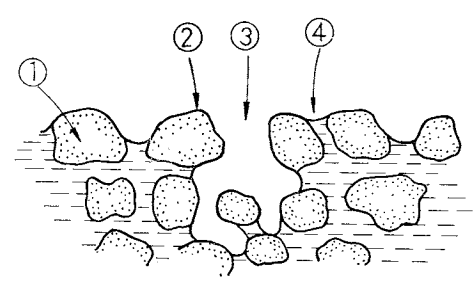

① Non-hygroscopic particle ② Dry surface
③ Vacant pore ④ Water meniscus

Fig. 1 Moisture distribution at the surface of non-hygroscopic granular beds during the constant drying rate period

* Received on June 29, 1967